IL-17A$^+$ group 2 innate lymphoid cells elicit mixed airway inflammation in chronic obstructive pulmonary disease

Cameron H. Flayer*, Angela L. Linderholm, Moyar Q. Ge, Maya Juarez, Lisa Franzi, Tina Tham, Melissa Teuber, Shu-Yi Liao, Michael Schivo, Brooks Kuhn, Amir Zeki, Angela Haczku**

UC Davis Lung Center, Pulmonary, Critical Care and Sleep Division, Department of Medicine, School of Medicine, University of California, Davis

*Now at Center for Immunology and Inflammatory Diseases, Massachusetts General Hospital

Correspondence: *Angela Haczku, MD, PhD, Professor of Medicine*

haczku@ucdavis.edu

Author Contributions: *C.H.F. planned, performed, and analyzed all experiments. A.L., L.F., T.T., M.J. M.T., M.S., B.K., and A.Z. planned and performed the clinical-related studies. M.Q.G. designed and tested the flow cytometry panels and together with C.H.F. planned and performed the mouse experiments. S.Y. performed the statistical and bioinformatic analyses. A.H. conceived and oversaw all aspects of the study. C.H.F., A.L., and A.H. wrote the manuscript.*

Support: *T32ES007059 and T32HL007013 to C.H.F; R21AI116121 and TRDRP27IR-0053 to A.H.*

Running Head: IL-17$^+$ILC2s denote COPD severity

Subject Category: 9.13 COPD: Pathogenesis

Word Count: 2995

Online Data Supplement: This article has an online data supplement, which is accessible from this issues table of contents online at www.atsjournals.org.

ABSTRACT

Rationale: Group 2 innate lymphoid cells (ILC2s) are important in asthma pathogenesis but their role in chronic obstructive pulmonary disease (COPD) has been controversial. COPD is associated with impaired function and expression of surfactant protein D (SP-D), a protective immune regulator in the lung.

Objectives: We aimed to establish the pathogenic significance of ILC2s and their regulation by SP-D in COPD.

Methods: Lung function, sputum and peripheral blood SP-D, immune cell and cytokine profile were evaluated in COPD and healthy subjects. Responsiveness to the air pollutant ozone (O_3) was studied in COPD-like SP-D$^{-/-}$ and conditional SP-D expressor mouse models. The effects of recombinant SP-D on isolated ILC2 gene and protein expression were investigated *in vitro*.

Measurements and Main Results: COPD patients with elevated sputum GATA3^{+}ILC2s (the ILC2^{high} group) showed significantly increased numbers of eosinophils, neutrophils and IL-17^{+}ILC2s. The ILC2 counts in ILC2^{high} (but not ILC2^{low}) sputum samples correlated with lung function, airway inflammation and leakage of degraded SP-D into the circulation. SP-D deficiency in O_3-exposed mice enhanced airway neutrophilia, promoted activation and RORγt and IL-17 expression by ILC2s in the lung. Recombinant SP-D suppressed both IL-13 and IL-17A in ILC2s *in vitro*. Adoptively transferred ILC2 induced neutrophilia in O_3-exposed Rag2/γc$^{-/-}$ mice in an IL-17A dependent manner.

Conclusions: IL-17A^{+}ILC2s were associated with a mixed neutrophilic and eosinophilic inflammation in COPD sputum and drove O_3-induced exacerbation of airway

inflammation in a mouse model. SP-D directly inhibited IL-17A^{+}ILC2s. Presence of IL-17A^{+}ILC2s may predict COPD severity.

Word Count: 244

Key Words: chronic obstructive pulmonary disease, innate lymphoid cell plasticity, IL-17A, surfactant protein-D

INTRODUCTION

While chronic obstructive pulmonary disease (COPD) continues to be a leading cause of mortality worldwide (1), the innate immune mechanisms central to the pathogenesis of this disease remain uncertain. A previously overlooked family of innate lymphoid cells (ILCs) emerged as pivotal in a variety of pulmonary diseases (2-4). This family was classified into subtypes as group 1 ILCs (ILC1s) that express T-bet and IFNγ, group 2 (ILC2s) that are defined by GATA3 and expression of IL-5 andIL-13, and group 3 (ILC3s) that are characterized by RORγt and IL-17A (2, 5). In asthma, group 2 innate lymphoid cells that produce IL-5 and IL-13 were singled out for their role in eosinophilic airway inflammation and lung function impairment (6, 7). In COPD however, it was suggested that ILC2s gain an ILC1-like phenotype, characterized by T-bet expression and IFNγ production (8). In patients with COPD, the frequency of peripheral blood ILC1s increased and correlated with disease severity, while the frequency of peripheral blood ILC2s was decreased (8). In a study of human lung tissue, COPD subjects showed an elevated frequency of ILC3s, not ILC1s nor ILC2s, compared to healthy controls (9). These conflicting data derived from different tissue compartments suggesting a role for ILCs in COPD, though the relevance of specific ILC subsets to disease severity and the underlying mechanisms of their activation remain uncertain.

The lung collectin surfactant protein-D (SP-D) is an immune protective epithelial derived soluble pattern recognition molecule, important in COPD pathogenesis (10-17). Bronchoalveolar lavage SP-D is diminished both in former and current smoker COPD subjects (18), while serum SP-D levels increase with lung function decline in (19). Mice genetically deficient in SP-D (SP-D$^{-/-}$) develop histologically and physiologically

quantifiable emphysema, and other pathological hallmarks of COPD (10) including spontaneous airway inflammation and activation of pulmonary innate immune cells. The relationship between SP-D and ILCs has never been characterized. Here we sought to clarify the role of ILCs in COPD severity and understand how SP-D impacts disease pathogenesis and ILC activation using sputum and peripheral blood samples from subjects with COPD. Acute exacerbation of airway inflammation in COPD is often caused by inhalation of the criteria air pollutant, ozone (O_3) (7, 11, 16, 18, 20-23). We therefore studied SP-D$^{-/-}$ mouse models exposed to O_3. Causality was investigated by adoptive transfer experiments with sorted ILC2s and direct treatment of these cells with recombinant SP-D *in vitro*.

METHODS

Human subjects

Patients with COPD (n=15) and non-smoking healthy volunteers (n=12) were recruited from the UC Davis pulmonary outpatient clinics. Details on inclusion and exclusion criteria are provided in the online supplement. Subjects that met eligibility criteria were consented and invited to enroll in the study. During a single study visit, the following procedures were conducted: review of medical record, physical examination, pulmonary function testing, health related quality of life surveys [modified medical research council scale (mMRC) and COPD assessment test (CAT)], venipuncture for collection of 20 mL blood, sputum induction by inhalation of 3% hypertonic saline, and 6-minute walk test. Healthy volunteers underwent all procedures except for the physical examination. For COPD patients, a physical examination, pulmonary function and 6-minute walk tests performed within 2 months of the initial study visit. This study was reviewed and approved by the University of California, Davis Institutional Review Board.

Sputum

10% Sputolysin reagent (MilliporeSigma, Burlington, MA) was added 1:1 weight/volume to induced sputum specimens. The sample was then placed in a 37°C shaking water bath for 15 minutes. Every 5 minutes, the sample was removed to be pipette mixed. Undiluted Sputolysin reagent was added as necessary if sample homogenization was poor. Sputum cells were strained through a 40 µm Olympus Advanced cell strainer [Genesee Scientific (San Diego, CA)] before cell count by the Countess™ Automated Cell Counter. Approximately $32x10^3$ cells were centrifuged at 500 rpm for 5 minutes onto a microscope slide, then stained via the Shandon Kwik-Diff staining kit (Thermo

Fisher Scientific, Waltham, MA). 2 cytospins were made for each subject. The remaining cells were apportioned for flow cytometry, while the sputum supernatant was aliquoted and snap frozen for storage at -80°C.

Cytospins were evaluated for the presence of macrophages/monocytes (MP), lymphocytes (LC), neutrophils (NP), eosinophils (EP), epithelial cells, and oral squamous cells. At minimum, 200 cells were counted per cytospin and differential cell percentages were averaged between cytospins for each subject. Sputum samples were deemed poor quality if >40% of the cytospin was squamous cells. This quality control criterium required n=4 healthy and n=5 COPD subjects to be excluded from the final analysis of sputum cells and supernatant, as well as ILC2^{high} and ILC2^{low} grouping.

Mice

The experimental animals used in this study were housed under pathogen-free conditions with free access to food and water on a 12 hour light-dark cycle. C57BL/6 wild-type (WT), Balb/c, and Rag2/γc$^{-/-}$ mice were obtained from The Jackson Laboratory (Sacramento, CA) and bred in house. SP-D$^{-/-}$ mice on the C57BL/6 background were a gift from Drs. Samuel Hawgood, University of California, San Francisco, and Francis Poulain, University of California, Davis and bred in house. The triple transgenic (*CCSP-rtTA*+, $(tetO)_7$-*rSP-D*+,*mSP-D*$^{-/-}$) mice were a generous gift of Dr. Jeffrey Whitsett (Cincinatti Childrens Hospital) were treated with doxycycline containing food pellets (25 mg/g; Harlan Tekland, Madison, WI) to induce the expression of rSP-D protein, and were bred in house. Experiments were conducted on 6-10 week old male mice. The University of California, Davis Institutional Animal Care and Use Committee approved the experimental protocol.

Mice were euthanized naïve or exposed to 3 ppm ozone (O_3) or air for 2 hours, then euthanized 12 hours later. Bronchoalveolar lavage (BAL) fluid and lungs were harvested to measure airway neutrophilia and lung ILC2s, respectively. BAL was obtained by instilling 2.7 mL phosphate-buffered saline (PBS) into the lungs (in 3 instillations) via tracheal cannula to collect cells and proteins of interest. Lungs were excised and single cell suspensions were made by digestion in Liberase™ [Roche (Basel, Switzerland)] for 40 minutes at 37° C. Cells were strained using a 70 µm cell strainer. Red blood cells were lysed, then strained a second time through a 70 µm strainer. BAL and lung cells were counted using the Countess™ Automated Cell Counter. Cell-free BAL supernatant was stored at -80°C for cytokine analysis.

For adoptive transfer studies, 250 µg αIL-17A or αIgG1 monoclonal antibodies were injected intraperitoneal (I.P.) into Rag2/γc$^{-/-}$ mice at 0, 24, and 48 hours. ILC2s were expanded *ex vivo* from donor WT lungs in 30 ng/mL IL-2+IL-7+IL-33 for 2 weeks, then 10^5 ILC2s were intravenously (I.V.) injected into the tail vein of recipient Rag2/γc$^{-/-}$ mice at 32 hours. 24 hours later (56 hours after the first monoclonal antibody injection), mice were exposed to air or O_3 and then euthanized 12 hours later. BAL was harvested to measure airway neutrophilia.

Flow cytometry antibodies, staining, and analysis

For mouse studies, Fixable Viability Stain 510 (BD Biosciences, San Jose, CA) was used following manufacturer's instructions. All anti-mouse antibodies were purchased from BioLegend (San Diego, CA), BD Biosciences (San Jose, CA), and eBioscience (San Diego, CA). A complete list of anti-mouse antibodies are provided in an online supplement.

For human studies, Zombie Green fixable viability kit (BioLegend, San Diego, CA) was used following manufacturer's instructions. All anti-human antibodies were purchased from BioLegend (San Diego, CA), BD Biosciences (San Jose, CA), and Miltenyi Biotec (Auburn, CA). A complete list of anti-human antibodies are provided in an online supplement.

Flow cytometric data was collected on a LSRFortessa™ [BD Biosciences, (San Jose, California)] with FACS Diva™ software [BD Biosciences, (San Jose, California)] and analyzed using FlowJo software [FlowJo, LLC (Ashland, Oregon)]. Cells were sorted using a FACSAria II™ [BD Biosciences, (San Jose, California)].

For intracellular cytokine detection from mouse ILC2s in the lung, cells were restimulated in 12.5 ng/mL phorbol 12-myristate 13-acetate (PMA, MilliporeSigma Burlington, MA), 500 ng/mL Ionomycin (MilliporeSigma, Burlington, MA) and 3 µM Monensin (MilliporeSigma, Burlington, MA) for 6 hours at 37° C. Lung cell suspensions were incubated in surface antigens for 20 minutes at 4° C in the dark. Cells were fixed and permeabilized using the FoxP3 perm/fix kit (BD Biosciences, San Jose, CA), then incubated in intracellular antigens for 30 minutes at 4° C in the dark. FMO or Lineage^{-} Thy1.2^{-} cells were used as technical controls.

For intracellular cytokine and transcription factor detection from human ILCs in blood and sputum, freshly isolated sputum and PBMC cell suspensions were incubated in surface antigens for 30 minutes on a shaker at room temperature in the dark. Cells were fixed and permeabilized using the BD Cytofix/Cytoperm kit (BD Biosciences, San Jose, CA), then incubated in intracellular antigens for 30 minutes on a shaker at room temperature in the dark. FMO cells were used as technical controls.

ILC2 culture (*ex vivo*)

Recombinant mouse IL-2, IL-7, and IL-33 were purchased from Peprotech (Rocky Hill, NJ).

ILC2 were isolated from the lungs of C57BL/6 and SP-D$^{-/-}$ mice as CD45^{+}Lineage^{-} Thy1.2^{+}CD127^{+}CD25^{+}ST2^{+} cells (lineage markers – CD3, CD4 CD5, CD11c, GR-1, B220, DX5) and cultured in non-treated U-bottom 96 well-plates. ILC2s were plated at 2,000 cells/well and stimulated in "ILC2 complete medium" (RPMI (ThermoFisher Scientific, Waltham, MA), 10% fetal bovine serum (Genesee Scientific, San Diego, CA), 1% penicillin/streptomycin (Genesee Scientific, San Diego, CA) and 10 ng/mL IL-2, IL-7, and IL-33). For culture experiments with recombinant SP-D, ILC2s were plated at 5,000 cells/well and expanded for 21 days in ILC2 complete medium, then rested in RPMI-alone for 16 hours. Following a rest period, ILC2s were stimulated for 3 days at 2,000 cells/well with cytokines and 0, 2, 10, or 20 µg/mL SP-D. At the time of harvest, cell free supernatant was collected for cytokine analysis (ELISA). Mouse recombinant SP-D (mrSP-D) was purchased from Sino Biological (Beijing, China).

ELISA and Luminex Assay

BAL KC was detected via Mouse CXCL1/KC DuoSet ELISA [cat# DY453, R&D Systems (Minneapolis, Minnesota)] following the manufacturer's protocol. IL-17A DuoSet ELISA (R&D Systems, Minneapolis, MN) was detected in cell-free ILC2 culture supernatant following the standard protocol. BAL cytokines were detected in naïve C57BL/6 and SP-D$^{-/-}$ mice via Luminex assay (Roche, Little Falls, NJ). The standard assay protocols supplied by the manufacturer were followed.

Human sputum IL-8 and SP-D was determined using a Luminex® magnetic bead-based premixed multiplex assay (R&D Systems, Minneapolis, MN) according to the manufacturer's protocol.

Western Blot

Sputum SP-D was detected via Native-PAGE western blot. Total protein in the BAL was quantified via Pierce BCA Protein Assay Kit (Thermo Fisher Scientific, Waltham, MA). 3.125 µg protein was run under native gel electrophoresis conditions using NuPAGE™ 1x Tris-Glycine Native Running Buffer (Thermo Fisher Scientific, Waltham, MA) at 150V for 120 minutes. The gel was transferred to a mini Nitrocellulose membrane using the iBlot® gel transfer mini stacks (Thermo Fisher Scientific, Waltham, MA). The membrane was probed with mouse anti-SP-D 1:1000 (in-house 10F6E12 monoclonal) followed by goat anti-mouse conjugated HRP 1:3000 (Santa Cruz Biotechnology, Santa Cruz, CA), then activated via Pierce™ ECL Western Blotting Substrate (Thermo Fisher Scientific, Waltham, MA.

qPCR

Total RNA was extracted from the whole lung with TRIzol Reagent (Thermo Fisher Scientific, Waltham, MA). cDNA was reverse-transcribed using the QuantiTect Reverse Transcription Kit (Qiagen, Hilden, Germany). qPCR was performed using Fast SYBR® Green Master Mix (Thermo Fisher Scientific, Waltham, MA) on a ViiA 7 Real-Time PCR System (Thermo Fisher Scientific, Waltham, MA). Fold change was calculated using the $\Delta\Delta C_t$ method, first normalizing values to *β-actin*, then to the treatment control. Primer sequences are included in the online supplement.

Data Analysis

Statistical analyses are indicated in each figure legend. Student's *t*-test, One-way ANOVA with Bonferroni's multiple comparison's test, Two-way ANOVA with Bonferroni's multiple comparisons test, and Linear Regression were applied using Graphpad Prism v7 (Graphpad Software Inc, La Jolla, CA) throughout the study. We performed regression correction for age. *$p<0.05$, **$p<0.01$, ***$p<0.001$, #$p<0.05$ were used to determine significance. Asterisks were used to denote statistically significant differences between groups indicated in the figure legends (i.e. healthy vs. COPD, WT vs. SP-D$^{-/-}$, and air vs. O_3). In O_3 exposure experiments utilizing C57BL/6 and SP-D$^{-/-}$ mice, hashmarks show interstrain differences (i.e. WT vs. SP-D$^{-/-}$). The human study was conducted over a period of 4 months, with a maximum of 3 subjects enrolled and processed per day. In the mechanistic mouse studies, experiments were independently performed 2-3 times.

RESULTS

Mixed neutrophilic and eosinophilic inflammation was associated with increased GATA3^{+}ILC2s in COPD sputum samples.

To examine the relationship between sputum ILCs and COPD severity, we evaluated lung function and sputum inflammatory and immune cell profiles in COPD and healthy, non-smoker subjects. Pre-bronchodilator forced expiratory volume in 1 second (FEV_1), forced vital capacity (FVC), % of predicted values and ratio of FEV_1 over FVC showed significantly decreased values in COPD subjects **(Fig. 1A)**. This corresponded to elevated lymphocyte, neutrophil and eosinophil counts in the sputum of

patients with COPD compared to healthy controls **(Fig. 1B-C)**. While sputum was predominated by neutrophils, in 7 of the 15 patients, there were elevated numbers of eosinophils present as well. We phenotypically characterized and measured ILCs by flow cytometry of sputum cell suspensions. We identified ILCs as live lymphocytes that were Lineage$^-$CD127$^+$ cells. Intracellular ILC expression of IL-5, IL-13, IL-17A, and IFNγ were all elevated in COPD subjects **(Fig. 1D).** ILC subtypes were identified by their transcription factor (T-bet$^+$, GATA3$^+$, and RORγt$^+$) expression. The proportions of the expression between the three different transcription factors were similar in healthy sputum samples but GATA3$^+$ILCs were the predominant ones in COPD patients. Compared to healthy subjects there were significantly more GATA3$^+$ILC2s in the sputum of COPD subjects **(Fig. 1E-F)**. These data suggested that a subset of COPD patients have mixed neutrophilic and eosinophilic inflammation in their airways in association with an increased count and proportion of GATA3$^+$ILCs (ILC2s).

COPD subjects with elevated sputum ILC2s (ILC2^{high}) had increased numbers of inflammatory cells and IL-17A-producing ILC2s.

To further assess the significance of the ILC2s in airway inflammation we stratified COPD patients into "ILC2^{high}" and "ILC2^{low}" groups by the upper limit of the 95% confidence interval of sputum ILC2 count for healthy controls. Thus, COPD subjects with ILC2s >1427 cells/mL sputum were ILC2^{high} (n=8), while subjects with ILC2s <1427 cells/mL sputum were ILC2^{low} (n=7) **(Fig. 2A).** ILC2^{high} subjects had significantly elevated sputum neutrophilia and eosinophilia compared to ILC2^{low} subjects **(Fig. 2B)**. Correlations between ILC2 counts and eosinophils, neutrophils and FEV_1 were made by linear regression using sputum samples from subjects with ILC2^{high}

sputum (dark blue circles, **Fig 2C**). These data suggest that the emergence of ILC2s in the sputum of COPD subjects is related to the severity of lung function decline, and sputum neutrophils and eosinophils. ILC2s drive airway inflammation through distinct mediators including IL-5 and IL-13 relevant to airway eosinophilia (2, 4, 6, 7, 9). On the other hand, RORγt ILC3s canonically produce IL-17A which plays a key role in initiating IL-8 production by epithelial cells to induce neutrophilia (2, 24, 25). There is evidence from prior mouse studies that ILC2s can co-express IL-13 and IL-17A under specific inflammatory conditions, and these cells were termed inflammatory ILC2s (26, 27). We therefore quantified GATA3^{+} ILC2 for IL-17A expression and found that ILC2^{high} subjects also displayed elevated GATA3^{+}IL-17A^{+} ILCs **(Fig. 2D)**. Thus, ILC2s could potentially contribute to the mixed neutrophilic and eosinophilic inflammation by co-expressing IL-5 or IL-13 with IL-17A.

Characteristics of healthy subjects and patients with ILC2^{low} and ILC2^{high} COPD sputum.

The characteristics of healthy subjects (n=12) and patients with COPD, stratified into ILC2^{low} (n=7) and ILC2^{high} (n=8) expressor groups are shown in **Table 1**. Subjects with COPD, regardless of ILC2 status were significantly older, had a history of smoking, had decreased oxygen saturation (SpO_2), increased modified medical research council scale (mMRC) and COPD assessment test (CAT) scores, and covered fewer meters in a 6-minute walk test compared to healthy volunteers. Peripheral blood neutrophil counts were also significantly increased in COPD patients compared to healthy controls. In addition, COPD ILC2^{high} patients had higher CAT scores compared to COPD ILC2^{low} patients. There was no difference in the cumulative number of pack years smoked

between ILC2^{high} and ILC2^{low} individuals, suggesting that overall smoke exposure wasn't playing a strong role in the clinical presentation of ILC2^{high} subjects **(Fig. E1)**. We did not find any difference in the peripheral blood differential cell counts between ILC2^{high} and ILC2^{low} individuals highlighting the importance of investigating the pulmonary compartment in the effort of identifying functionally relevant disease endotypes in COPD.

The age range did not differ significantly within the COPD group between ILC2^{high} and ILC2^{low} patients **(Table 1).** Nonetheless, we wanted to verify if age played a significant role in the observed effects of high ILC2 counts. Using multiple linear regression analysis, we found that FEV_1, sputum neutrophil and eosinophil counts remained significantly correlated with sputum ILC2s while the CAT scores lost statistical significance (p=0.051) after correction for age **(Table 2)**. Of note, FVC did not correlate with ILC2s neither before nor after age adjustment. These results suggest that ILC2s in the airways have a potential pathogenic significance in driving mixed neutrophilic and eosinophilic airway inflammation and the obstructive component of lung function impairment in COPD patients.

ILC2 counts in ILC2^{high} (but not ILC2^{low}) sputum samples are correlated with SP-D release to sputum and serum SP-D leakage.

We previously found that airway SP-D levels in the BAL significantly diminished in subjects with COPD, proportionately with disease severity (18). Meanwhile, total lack of SP-D in the lung of gene deficient mice showed spontaneous airway inflammation, activation of pulmonary innate immune cells and COPD-like pathological features such as emphysema (10-12, 14, 17, 28), suggesting that high levels of SP-D are protective.

We were surprised to find therefore, that in the sputum of COPD subjects there were significantly higher concentrations of SP-D (measured by Luminex) compared to healthy controls. Sputum SP-D was even more elevated in ILC2^{high} than ILC2^{low} COPD patients **(Fig. 3A)**. Since the tertiary and quaternary oligomeric structures of SP-D are sensitive to degradation due to oxidative stress in the chronically inflamed airways (21, 29), sputum may contain an increased amount of the much smaller de-oligomerized molecule, which can also readily leak into the circulation. Indeed, we found that corresponding with increased total SP-D levels both in the sputum and serum of COPD subjects, there was a significant degradation of the native SP-D structure **(Fig. 2B)**. Further, sputum ILC2 counts in the ILC2^{high} group correlated with SP-D concentrations both in the sputum and serum suggesting that greater airway inflammation is associated with greater degradation of SP-D **(Fig. 2C).** This is confirmed by the positive correlations of total sputum SP-D with the pro-eosinophilic CCL24 and IL-5 in the ILC2^{high} (but not ILC2^{low}) group **(Fig. 2D)**.

SP-D deficiency promoted inflammation and ILC2 activation in the lung.

While SP-D was previously suggested to play an important role in COPD pathogenesis and capable of inhibiting immune cells (12, 16), its effects on ILC2s have never been evaluated. Because the neutrophils play a prominent role in the pathogenesis of COPD (30), we hypothesized that SP-D$^{-/-}$ mice would also spontaneously develop airway neutrophilia. At 6 weeks of age, SP-D$^{-/-}$ mice showed marked BAL neutrophilia that was completely absent in C57BL/6 wild-type (WT) mice **(Fig. 4A)**. This was accompanied by significantly increased BAL KC, the mouse equivalent of IL-8 **(Fig. 4B)**.

Compared to WT mice, SP-D$^{-/-}$ displayed significantly elevated mRNA expression of *cxcl1*, *il1rl1* and *Il33,* the main growth factor for ILC2 (2) **(Fig. 4C)**. We thus hypothesized that ILC2s are elevated in the SP-D$^{-/-}$ lung. ILCs derived from whole lung homogenate were Lineage^{-}Thy1.2^{+}, further characterized as ILC2s by expression of CD127 and ST2 (the IL-33 receptor) **(Fig. 4D)**. SP-D$^{-/-}$ mice had significantly more lung ILC2s than WT mice, suggesting that ILC2s were a direct target of SP-D immunomodulation **(Fig. 4E)**. Intracellular IL-13 was measured and more highly expressed in ILC2s from SP-D$^{-/-}$ mice **(Fig. 4F)**.

To study if these changes were secondary to the COPD-like pathologies in the SP-D$^{-/-}$ mice or specifically due to lack of SP-D, we studied conditional SP-D expressing (*Ccsp-rtTA*+(*tetO*)$_7$-*rSftpd*+*mSftpd*$^{-/-}$) mice in which expression of the SP-D gene was tied to a tetracycline promoter in club cells of the lung (28). Doxycycline diet was withdrawn on day 0. Mice were studied on days 0 and 10. SP-D was detected in the BAL supernatant (by western blot) and cytospins of BAL cells from corresponding samples were assessed **(Fig. 4G)**. Conditional elimination of SP-D expression led to airway neutrophilia and activation of lung ILC2s and intracellular IL13 expression as quantified by FACS analysis **(Fig. 4H)**. These data suggested that ILC2 activation in the lung may be a direct result of the absence of SP-D.

SP-D suppressed the emergence of IL-13 and IL-17A-producing ILC2s in the lung.

Given that ILC2^{high} COPD subjects displayed significant sputum neutrophilia and elevated IL-17A+ ILCs, and SP-D$^{-/-}$ mice had elevated airway neutrophils, we hypothesized that SP-D regulated IL-17A in ILC2s. We FACS-sorted Lineage^{-}

Thy1.2^{+}CD25^{+}ST2^{+} cells **(Fig. 5A)**. Purity of ILC2 sorts were confirmed by flow cytometry immediately following ILC2 isolation (**Fig. E2** in the online data supplement). Analysis of Gata 3 and IL-13 expression demonstrated significantly increased expression of IL-13 in SP-D$^{-/-}$ mice while rSP-D dose-dependently inhibited IL-13 expression **(Fig. 5B, C and D)**. ILC2s were also sorted for RORγt expression and shown to be increased significantly in SP-D$^{-/-}$ mice **(Fig. 5E, F, G and H)**. Strikingly, SP-D$^{-/-}$ ILC2s secreted IL-17A that was completely absent from WT ILC2s and was dose-dependently inhibited by rSP-D *ex vivo* **(Fig. 5I and J)**. These results indicate that SP-D controls IL-17A expression in lung ILC2s.

SP-D deficiency predisposed mice to O_3-induced airway neutrophilia and lung ILC2 activation.

The progressive nature of COPD is frequently aggravated by exacerbations. These short bouts of severe symptoms are driven, in part, by the presence of highly activated neutrophils in the airways (30, 31). COPD patients are uniquely susceptible to neutrophilic exacerbation driven by the air pollutant ozone (O_3) (22, 23). We hypothesized that a trigger of COPD exacerbation would enhance the IL-17A signal in lung ILC2s of SP-D$^{-/-}$ mice. WT and SP-D$^{-/-}$ mice were exposed to 3 ppm O_3 for 2 hours, then studied 12 hours later. SP-D$^{-/-}$ mice showed significantly heightened airway neutrophilia after O_3 exposure compared to WT mice **(Fig. 6A-B)**. Likewise, BAL KC was induced by O_3 exposure, elevated in the absence of SP-D **(Fig. 6C)**. We next examined the impact of O_3 on lung ILC2s. We found that SP-D$^{-/-}$ ILC2s increased in the lung following O_3 exposure **(Fig. 6D)**. In other experiments on the SP-D$^{-/-}$ lungs we identified ILC2s by ST2 expressing. Here we had to use GATA3 because O_3 exposure

reduced the expression of ST2 on lung ILC2s in the exposed mice **(Fig. 6E)**. Concomitant to the ST2 reduction, O_3 significantly increased the ST2^{low}RORγt^{+} ILC2s in the lung of SP-D$^{-/-}$ mice **(Fig. 6F)**. These data suggested that a trigger of COPD exacerbation could enhance the IL-17A signal in lung ILC2s.

ILC2 derived IL-17A was essential for ozone-induced neutrophilia in mice

Because O_3 caused neutrophilic airway inflammation and induced expression of RORγt^{+} in lung ILC2s, we investigated if the IL-17A producing capability of SP-D$^{-/-}$ ILC2s was enhanced in this model. In SP-D$^{-/-}$ mice, O_3 increased the proportion of lung ILC2s that expressed IL-17A compared to WT controls **(Fig. 7A)**. This was accompanied by an O_3-induced increase in the number of IL-17A^{+}IL-13^{+}ILC2s in SP-D$^{-/-}$, but not WT mice **(Fig. 7B)**. Similarly, the proportion of IL-17A^{+} ILCs that co-expressed GATA3 and RORγt^{+} was significantly increased by O_3 in SP-D$^{-/-}$, but not WT mice **(Fig. 7C)**. To understand if ILC2-derived IL-17A was important to airway neutrophilia, we employed Rag2/γc$^{-/-}$ mice (on the Balb/c background) lacking innate and adaptive lymphocytes. Compared to Balb/c mice, Rag2/γc$^{-/-}$ mice exhibited reduced airway neutrophilia, which could be restored with adoptive transfer of ILC2s expanded *ex vivo* prior to O_3 **(Fig. 7D and E)**. Recipient Rag2/γc$^{-/-}$ mice given ILC2s and injected with αIL-17A had less airway neutrophilia, expressed lower CXCL-1 and higher IL-27 compared to animals receiving αIgG1 control **(Fig. 7F and G)**. These data suggested that SP-D plays a key role in regulating the development of highly proinflammatory dual-positive IL-13^{+}IL-17A^{+} ILC2s in the lung, and further that this process is required for airway neutrophilia.

DISCUSSION

Here we establish a mechanistic link between SP-D and lung ILC2s, complementing our clinical studies on severely ill COPD subjects with elevated sputum ILC2s and degraded SP-D. ILC2^{high} subjects with COPD had decreased FEV_1, increased CAT scores, and enhanced sputum neutrophilia and eosinophilia compared to ILC2^{low} and healthy subjects. This was associated with the emergence of ILCs co-expressing IL-13 with IL-17A. Lack of SP-D expression in the mouse lung led to IL-17A production in lung ILC2s that was associated with airway neutrophilia. SP-D$^{-/-}$ mice showed heightened susceptibility to O_3-induced neutrophilia, with increased numbers of IL-17A^{+} lung ILC2s. These data demonstrate that sputum ILC2s may be a good predictor of disease severity in COPD, especially when mixed neutrophilic and eosinophilic inflammation is observed.

Initially, we set out to define the role of ILCs in the disease severity of COPD. Surprisingly, we found that ILCs expressing GATA3 were increased in the sputum of subjects with COPD compared to healthy controls. Within the COPD group however, we noticed that some patients clearly showed elevated ILC2s/mL sputum, while others had similar levels when compared to healthy controls. Thus, to gain deeper insight into the relevance of ILC2s in COPD, we stratified subjects into ILC2^{high} and ILC2^{low} subgroups based on the upper limit of the 95% confidence interval in healthy controls. The ILC2^{high} group had more severe disease than ILC2^{low} subjects with COPD based on lung function, CAT score, and sputum inflammation. Since ILC2s were previously recognized for their role in Type 2 immunity (2, 6), it was unexpected to see them elevated in the

sputum of COPD subjects showing a neutrophil-high clinical presentation. However, the ILC2^{high} patients displayed elevated sputum neutrophils as well as eosinophils, which wasn't statistically apparent when viewing the COPD group as a whole. ILCs expressing IL-13 in combination with IL-17A in these subjects suggested that ILC2s gained a dual-functional phenotype, contributing to the mixed neutrophilic and eosinophilic inflammatory profile. These data suggest a novel role for ILC2s, expressing their canonical cytokines IL-5 and IL-13 in combination with IL-17A, as a highly pro-inflammatory population in severe COPD.

Prior work by Silver et al. showed that ILC1s increased and ILC2s decreased in the peripheral blood of patients with COPD, while De Grove et al. demonstrated that ILC2s were decreased and ILC3s increased in the lung tissue of COPD (8, 9). Here we studied ILCs in the sputum, and we used transcription factors to define ILCs as ILC1s, ILC2s, and ILC3s. This tissue specificity and slight modification of gating strategy could explain the discrepancies between our studies. Moreover, the observation that ILC2^{high} subjects had significant eosinophilia compared to healthy controls suggest that our cohorts were clinically different.

We wondered how ILC2s could gain IL-17A functionality. SP-D was previously recognized as an important immunomodulator in the pathogenesis of COPD (10, 18, 28, 32-34). In our clinical study, we found that while overall SP-D concentrations were increased the sputum of subjects with COPD, the native structure of the protein was unraveled. Because the SP-D structure is subject to post-translational modifications that render its immunomodulatory capabilities nonfunctional (21, 29), we propose that nonfunctional SP-D in the ILC2^{high} group led to enhanced activation of ILC2s and a

mixed cytokine profile of ILCs in the sputum. To study the mechanisms of SP-D and ILC2-acquired IL-17A, we turned to mouse and *ex vivo* models.

We utilized SP-D$^{-/-}$ mice that spontaneously develop the histological and inflammatory features of COPD (10). Lack of SP-D led to increased numbers of ILC2s and were capable of IL-17A production *ex vivo*. IL-17A secretion was dose-dependently inhibited by recombinant SP-D, suggesting that lack of functional SP-D in the sputum of COPD patients could lead to enhanced numbers of IL-17A-expressing ILC2s. Using the air pollutant O_3 as a trigger for neutrophilic exacerbation, we found that activation of IL-17A expressing ILC2s was enhanced in the absence of SP-D. This activation was necessary for the observed airway neutrophilia, linking SP-D and ILC2s to the clinical features observed in our COPD cohort. Since the regulation of ILC2s (35, 36) is poorly understood and the vast majority of SP-D in the body is produced in the lung, these data shed light on lung-specific control of ILC2 activity. Other chronic inflammatory lung diseases characterized by impaired SP-D may predispose individuals to ILC2-mediated adverse pathologies. It is possible that therapeutic interventions to elevate functional SP-D expression may impact this pathway.

As ILC2s are among the first to respond to inhaled pathogens and environmental stressors in the lung, how they initiate the inflammatory response may have a disproportionately large implication to disease pathogenesis. In COPD, lack of functional SP-D may skew ILC2s to produce IL-17A in combination with IL-5 and IL-13, leading to a mixed inflammatory profile and more severe disease.

ACKNOWLEDGEMENTS

The authors thank members of the Haczku laboratory for their suggestions during laboratory meetings and assistance in technical aspects of the study: Erik Larson, Sarah Killingbeck, Jessica-Miranda Bustamante, and Sean Ott. The authors thank Abigail Spinner in the Clinical Laboratory at the UC Davis California National Primate Research Center for her expertise in flow cytometry and assistance with FACS experiments. We also thank the UC Davis Air Pollution Journal Club led by Dr. Laura Van Winkle for their critical review of the manuscript. The authors gratefully acknowledge the generous gifts of the conditional SP-D expressor mice from the laboratory of Dr. Jeffrey Whitsett (Cincinnati Childrens Hospital); and the SP-D$^{-/-}$ mice from the laboratory of Dr. Samuel Hawgood (UCSF) and Francis Poulain (UC Davis).

COMPETING FINANCIAL INTERESTS

The authors declare no competing financial interests.

ABBREVIATIONS

Chronic Obstructive Pulmonary Disease (COPD)

Surfactant Protein-D (SP-D)

Innate Lymphoid Cell (ILC)

Group 1 Innate Lymphoid Cell (ILC1)

Group 2 Innate Lymphoid Cell (ILC2)

Group 3 Innate Lymphoid Cell (ILC3)

Forced Expiratory Volume in one second (FEV_1)

Forced Vital Capacity (FVC)

Global Initiative for Chronic Obstructive Lung Disease (GOLD)

Pulmonary Function Testing (PFT)

Modified Medical Research Council scale (mMRC)

COPD Assessment Test (CAT)

Macrophage/monocyte (MP)

Lymphocyte (LC)

Neutrophil (NP)

Eosinophil (EP)

C57BL/6 Wild-type (WT)

Bronchoalveolar Lavage (BAL)

Ozone (O_3)

Phosphate-buffed Saline (PBS)

Mouse Recombinant SP-D (rSP-D)

Specific Oxygen (SpO_2),

REFERENCES

1. Burney PG, Patel J, Newson R, Minelli C, Naghavi M. Global and regional trends in COPD mortality, 1990-2010. *Eur Respir J* 2015; 45: 1239-1247.
2. Artis D, Spits H. The biology of innate lymphoid cells. *Nature* 2015; 517: 293-301.
3. Blomme EE, Provoost S, De Smet EG, De Grove KC, Van Eeckhoutte HP, De Volder J, Hansbro PM, Bonato M, Saetta M, Wijnant SR, Verhamme F, Joos GF, Bracke KR, Brusselle GG, Maes T. Quantification and role of innate lymphoid cell subsets in Chronic Obstructive Pulmonary Disease. *Clinical & Translational Immunology* 2021; 10: e1287.
4. Yashiro T, Moro K. Crossing the valley of death: Toward translational research regarding ILC2. *Allergol Int* 2023; 72: 187-193.
5. Bal SM, Golebski K, Spits H. Plasticity of innate lymphoid cell subsets. *Nature Reviews Immunology* 2020; 20: 552-565.
6. McKenzie AN. Type-2 innate lymphoid cells in asthma and allergy. *Ann Am Thorac Soc* 2014; 11 Suppl 5: S263-270.
7. Yang Q, Ge MQ, Kokalari B, Redai IG, Wang X, Kemeny DM, Bhandoola A, Haczku A. Group 2 innate lymphoid cells mediate ozone-induced airway inflammation and hyperresponsiveness in mice. *J Allergy Clin Immunol* 2016; 137: 571-578.
8. Silver JS, Kearley J, Copenhaver AM, Sanden C, Mori M, Yu L, Pritchard GH, Berlin AA, Hunter CA, Bowler R, Erjefalt JS, Kolbeck R, Humbles AA. Inflammatory triggers associated with exacerbations of COPD orchestrate plasticity of group 2 innate lymphoid cells in the lungs. *Nat Immunol* 2016; 17: 626-635.

9. De Grove KC, Provoost S, Verhamme FM, Bracke KR, Joos GF, Maes T, Brusselle GG. Characterization and Quantification of Innate Lymphoid Cell Subsets in Human Lung. *PLoS One* 2016; 11: e0145961.

10. Wert SE, Yoshida M, LeVine AM, Ikegami M, Jones T, Ross GF, Fisher JH, Korfhagen TR, Whitsett JA. Increased metalloproteinase activity, oxidant production, and emphysema in surfactant protein D gene-inactivated mice. *Proc Natl Acad Sci U S A* 2000; 97: 5972-5977.

11. Kierstein S, Poulain FR, Cao Y, Grous M, Mathias R, Kierstein G, Beers MF, Salmon M, Panettieri RA, Jr., Haczku A. Susceptibility to ozone-induced airway inflammation is associated with decreased levels of surfactant protein D. *Respir Res* 2006; 7: 85.

12. Haczku A, Cao Y, Vass G, Kierstein S, Nath P, Atochina-Vasserman EN, Scanlon ST, Li L, Griswold DE, Chung KF, Poulain FR, Hawgood S, Beers MF, Crouch EC. IL-4 and IL-13 form a negative feedback circuit with surfactant protein-D in the allergic airway response. *J Immunol* 2006; 176: 3557-3565.

13. Haczku A, Vass G, Kierstein S. Surfactant protein D and asthma. *Clin Exp Allergy* 2004; 34: 1815-1818.

14. Hortobágyi L, Kierstein S, Krytska K, Zhu X, Das AM, Poulain F, Haczku A. Surfactant protein D inhibits TNF-alpha production by macrophages and dendritic cells in mice. *J Allergy Clin Immunol* 2008; 122: 521-528.

15. Forbes LR, Haczku A. SP-D and regulation of the pulmonary innate immune system in allergic airway changes. *Clin Exp Allergy* 2010; 40: 547-562.

16. Ge MQ, Kokalari B, Flayer CH, Killingbeck SS, Redai IG, MacFarlane AWt, Hwang JW, Kolupoti A, Kemeny MD, Campbell KS, Haczku A. Cutting Edge: Role of NK Cells and Surfactant Protein D in Dendritic Cell Lymph Node Homing: Effects of Ozone Exposure. *J Immunol* 2016; 196: 553-557.

17. Haczku A. Protective role of the lung collectins surfactant protein A and surfactant protein D in airway inflammation. *J Allergy Clin Immunol* 2008; 122: 861-879; quiz 880-861.

18. Sims MW, Tal-Singer RM, Kierstein S, Musani AI, Beers MF, Panettieri RA, Haczku A. Chronic obstructive pulmonary disease and inhaled steroids alter surfactant protein D (SP-D) levels: a cross-sectional study. *Respir Res* 2008; 9: 13.

19. Dalgård C, Wang F, Titlestad IL, Kyvik KO, Vestbo J, Sorensen GL. Increased serum SP-D in identification of high-risk smokers at high risk of COPD. *American Journal of Physiology-Lung Cellular and Molecular Physiology* 2021; 320: L1005-L1010.

20. Lee YG, Lee PH, Choi SM, An MH, Jang AS. Effects of Air Pollutants on Airway Diseases. *Int J Environ Res Public Health* 2021; 18.

21. Yousefi S, Sharma SK, Stojkov D, Germic N, Aeschlimann S, Ge MQ, Flayer CH, Larson ED, Redai IG, Zhang S, Koziol-White CJ, Karikó K, Simon HU, Haczku A. Oxidative damage of SP-D abolishes control of eosinophil extracellular DNA trap formation. *J Leukoc Biol* 2018; 104: 205-214.

22. Khaniabadi YO, Hopke PK, Goudarzi G, Daryanoosh SM, Jourvand M, Basiri H. Cardiopulmonary mortality and COPD attributed to ambient ozone. *Environ Res* 2017; 152: 336-341.

23. Medina-Ramón M, Zanobetti A, Schwartz J. The effect of ozone and PM10 on hospital admissions for pneumonia and chronic obstructive pulmonary disease: a national multicity study. *Am J Epidemiol* 2006; 163: 579-588.

24. Withers DR, Hepworth MR, Wang X, Mackley EC, Halford EE, Dutton EE, Marriott CL, Brucklacher-Waldert V, Veldhoen M, Kelsen J, Baldassano RN, Sonnenberg GF. Transient inhibition of ROR-gammat therapeutically limits intestinal inflammation by reducing TH17 cells and preserving group 3 innate lymphoid cells. *Nat Med* 2016; 22: 319-323.

25. van de Pavert SA, Ferreira M, Domingues RG, Ribeiro H, Molenaar R, Moreira-Santos L, Almeida FF, Ibiza S, Barbosa I, Goverse G, Labao-Almeida C, Godinho-Silva C, Konijn T, Schooneman D, O'Toole T, Mizee MR, Habani Y, Haak E, Santori FR, Littman DR, Schulte-Merker S, Dzierzak E, Simas JP, Mebius RE, Veiga-Fernandes H. Maternal retinoids control type 3 innate lymphoid cells and set the offspring immunity. *Nature* 2014; 508: 123-127.

26. Huang Y, Guo L, Qiu J, Chen X, Hu-Li J, Siebenlist U, Williamson PR, Urban JF, Jr., Paul WE. IL-25-responsive, lineage-negative KLRG1(hi) cells are multipotential 'inflammatory' type 2 innate lymphoid cells. *Nat Immunol* 2015; 16: 161-169.

27. Zhang K, Xu X, Pasha MA, Siebel CW, Costello A, Haczku A, MacNamara K, Liang T, Zhu J, Bhandoola A, Maillard I, Yang Q. Cutting Edge: Notch Signaling Promotes the Plasticity of Group-2 Innate Lymphoid Cells. *J Immunol* 2017; 198: 1798-1803.

28. Zhang L, Ikegami M, Dey CR, Korfhagen TR, Whitsett JA. Reversibility of pulmonary abnormalities by conditional replacement of surfactant protein D (SP-D) in vivo. *J Biol Chem* 2002; 277: 38709-38713.

29. Guo CJ, Atochina-Vasserman EN, Abramova E, Foley JP, Zaman A, Crouch E, Beers MF, Savani RC, Gow AJ. S-nitrosylation of surfactant protein-D controls inflammatory function. *PLoS Biol* 2008; 6: e266.

30. Butler A, Walton GM, Sapey E. Neutrophilic Inflammation in the Pathogenesis of Chronic Obstructive Pulmonary Disease. *Copd* 2018; 15: 392-404.

31. López-Campos JL, Tan W, Soriano JB. Global burden of COPD. *Respirology* 2016; 21: 14-23.

32. Moré JM, Voelker DR, Silveira LJ, Edwards MG, Chan ED, Bowler RP. Smoking reduces surfactant protein D and phospholipids in patients with and without chronic obstructive pulmonary disease. *BMC Pulm Med* 2010; 10: 53.

33. Akiki Z, Fakih D, Jounblat R, Chamat S, Waked M, Holmskov U, Sorensen GL, Nadif R, Salameh P. Surfactant protein D, a clinical biomarker for chronic obstructive pulmonary disease with excellent discriminant values. *Exp Ther Med* 2016; 11: 723-730.

34. Bowler RP. Surfactant protein D as a biomarker for chronic obstructive pulmonary disease. *Copd* 2012; 9: 651-653.

35. Duerr CU, McCarthy CD, Mindt BC, Rubio M, Meli AP, Pothlichet J, Eva MM, Gauchat JF, Qureshi ST, Mazer BD, Mossman KL, Malo D, Gamero AM, Vidal SM, King IL, Sarfati M, Fritz JH. Type I interferon restricts type 2

immunopathology through the regulation of group 2 innate lymphoid cells. *Nat Immunol* 2016; 17: 65-75.

36. Kudo F, Ikutani M, Seki Y, Otsubo T, Kawamura YI, Dohi T, Oshima K, Hattori M, Nakae S, Takatsu K, Takaki S. Interferon-γ constrains cytokine production of group 2 innate lymphoid cells. *Immunology* 2016; 147: 21-29.

Figure Legends

Figure 1. Mixed neutrophilic and eosinophilic inflammation in COPD sputum was associated with increased GATA3$^+$ILC2s. (A) Pre-bronchodilator forced expiratory volume in 1 second (FEV_1) and forced vital capacity (FVC), % of predicted values and ratio of FEV_1 over FVC of healthy and COPD subjects. **(B)** Cytospins of induced sputum cells from healthy (top left) and COPD subjects were stained with Kwik-Diff. The enlarged images illustrate a macrophage surrounded by neutrophils; the insert shows a multi-nucleated macrophage, a neutrophil and two eosinophilic granulocytes. **(C)** Macrophages, lymphocytes, neutrophils, eosinophils and epithelial cells (not shown) were counted on at least 4 high-powered fields of 2 cytospin slides/subject. Percent differential counts were multiplied by the total sputum cell count/mL. **(D)** Identification of innate lymphoid cells [ILCs; live Lineage$^-$CD127$^+$ (lineage markers: CD3, CD14, CD16, CD19, CD20, CD56)] by flow cytometry in sputum and intracellular expression of IL-5, IL-13, IL-17A, and IFNγ (ILCs/mL sputum). Dotted line indicates background. **(E)** Pie chart average % values of ILCs that were T-bet$^+$, GATA3$^+$, and RORγt$^+$. **$p<0.01$ (healthy (n=12) vs. COPD (n=15). **(F)** Counts of T-bet$^+$ (ILC1s), GATA3$^+$ (ILC2s), and RORγt$^+$ (ILC3s), cells/mL sputum. **(A, C-D, F):** Mean±SEM of n=12-16 healthy, n=15-20 COPD. *$p<0.05$, **$p<0.01$, ***$p<0.001$, Mann-Whitney multiple comparisons test with FDR.

Figure 2. COPD subjects with elevated sputum ILC2s (ILC2^{high}) have increased numbers of inflammatory cells and IL-17+ ILC2s. (A): COPD subjects were stratified according to their sputum ILC2 counts into ILC2^{low} (light blue circles) and ILC2^{high} (dark blue circles) groups, determined by the upper limit of the 95% confidence interval (1500

cells/mL sputum; dotted line). 9 of 15 COPD subjects had ILC2^{high} Sputum. **(B):** Sputum neutrophil and eosinophil counts of ILC2^{low} (light blue bar) and ILC2^{high} (dark blue bar) subjects (cells/mL sputum). **(C):** Correlations between ILC2 counts (dark blue circles) and eosinophils, neutrophils and FEV_1 were made by linear regression using sputum samples from subjects with ILC2^{high} sputum (r: Pearson's correlation coefficient). ILC2^{low} sputum samples (light blue circles) were not included in the correlation. **(D):** ILC2s gated on GATA3^{+} expression from [ILCs; live Lineage^{-}CD127^{+} (lineage markers: CD3, CD14, CD16, CD19, CD20, CD56)] were assessed for intracellular IL-17. **(A-B, D):** Mean±SEM of n=15-20 COPD patients. **(B, D):** Mean±SEM of ILC2^{low} and ILC2^{high} samples from n=7 and n=8 COPD subjects, respectively; * $p<0.05$, ** $p<0.01$, Mann-Whitney multiple comparisons test with FDR.

Figure 3. ILC2 counts in ILC2^{high} (but not ILC2^{low}) sputum samples correlated with SP-D release to sputum and serum SP-D leakage. (A) SP-D measured by Luminex® assay in the cell free supernatant of sputum (left panel) and serum samples from healthy subjects and COPD patients with ILC2^{low} and ILC2^{high} sputum (ng/mL). Mean±SEM of n=12 healthy, and ILC2^{low} and ILC2^{high} samples from n=7 and n=8 COPD subjects, respectively. **p=0.003 Sputum; **p=0.007 Serum; Kruskal Wallis multiple comparison. **(B)** SP-D Native gel electrophoresis (Representative sputum samples, bottom panel) using an in-house developed mouse anti-SPD (1µg; 106FE12 monoclonal), followed by goat anti-mouse conjugated HRP 1:3000. De-oligomerized low molecular weight components of SP-D streak down the native gel, while the intact (native) SP-D molecule stays on the top. Corresponding Luminex® sputum and serum samples denote the extent of serum leakage of SP-D from the same individuals. **(C)**

Correlations of total serum (top) and sputum (bottom) SP-D and sputum ILC2 counts in ILC2^{high} (dark blue circles) sputum samples from COPD subjects. **(D)** Correlations of total SP-D and CCL24 (Eotaxin 2, top panel) and IL-5 (measured by Luminex®) in sputum supernatant. **(C-D):** Linear regression (r: Pearson's correlation coefficient); only ILC2^{high} samples included. There was no correlation observed in the ILC2^{low} samples.

Figure 4. Effect of SP-D deficiency on airway inflammation and lung ILC2s. (A) 8-12 weeks old age- and sex matched SP-D-/- and wild type (C57BL/6) littermates were studied for BAL and lung cells and cytokines. Cytospins of BAL cells were stained with Kwik-Diff and assessed for the presence of macrophages (MP), eosinophils (EP), neutrophils (NP) and lymphocytes (LC). Differential BAL cell counts (x10^2) were calculated using the total BAL cells. **(B)** Cell-free BAL supernatant was assessed by ELISA for KC concentration (pg/mL). **(C)** Total lung RNA was extracted and processed for cxcl1, il1rl1, ifng and il33 mRNA expression by qPCR. **(**fold change over C57BL/6 average ctrl values). **(D)** Gating strategy for mouse lung ILCs: live Lin$^-$Thy1.2$^+$ cells (lineage markers – CD3, CD4 CD5, CD11c, GR-1, B220, DX5). Representative scatter plots showing the proportion of lung ILCs in that were CD127$^+$ST2$^+$ (ILC2s). **(E)** Quantification of lung ILC2s (% of lung lymphocytes). **(F):** Intracellular IL-13 expression by lung ILC2s. Mean±SEM of n=6-11 **(A)**, n=6-8 **(B, C, E)**; *p<0.05 or **p<0.01, Student's *t*-test (C57Bl/6 vs. SP-D$^{-/-}$). **(G):** In conditional SP-D expressing (*Ccsp-rtTA*+(*tetO*)$_7$-*rSftpd*+*mSftpd*$^{-/-}$) mice, expression of the SP-D gene was tied to a tetracycline promoter in club cells of the lung. Doxycycline diet was removed on day 0; mice were studied on days 0 and 10. SP-D was detected in the BAL supernatant (western blot) and cytospins of BAL cells from corresponding samples were assessed

(Kwik-Diff, 400x). **(H):** Elimination of SP-D expression led to airway neutrophilia and activation of lung ILC2s (FACS analysis). Quantification of lung ILC2s and IL-13$^+$ ILC2s (% of lung lymphocytes) n=3-4.

Figure 5. SP-D suppressed IL-13 and IL-17A co-expressing inflammatory ILC2s. (A): ILC2s (live CD45$^+$Lineage$^-$Thy1.2$^+$ST2$^+$CD25$^+$ cells) were freshly isolated from mouse lung for mRNA analysis, or *in vitro* culture in 10 ng/mL IL-2+7+33. **(B, H):** Gene expression (qPCR) analysis of freshly isolated ILC2s (log fold change over C57BL/6 wild type control). **(C, I):** IL-13 and IL-17A of ILC2 supernatant after 7-day culture with 10 ng/mL IL-2+7+33 (ELISA; pg/mL). **(D, J):** IL-13 and IL-17A of ILC2 culture supernatant after addition of mrSP-D for 3 days (ELISA; pg/mL). **(E)** Overlay of RORγt expression (MFI) on lung ILC2s. **(F)** RORγt MFI in lung ILC2s (ratio over C57BL/6). **(G):** Quantification of lung RORγt$^+$ ILC2s (% of lung lymphocytes). Mean **(B, H)**, quartiles (boxes) and range (whiskers) **(C, F, G, I)**, or mean±SEM **(D, J)** of n=2-3 from 3-4 pooled mice per point, n=4-11 **(C)**, n=7-9 **(D, I, J)**, n=7-8 **(E-G)**, n=7-9 **(I)**; *p<0.05, **p<0.01, ***p<0.001 (**C, F, G, I:** Student's *t*-test; **D, J:** One-way ANOVA with Bonferroni correction).

Figure 6. SP-D deficiency enhanced O_3-induced airway neutrophilia and lung ILC2 activation. (A) Mice were exposed to 3 ppm O_3 for 2 hours, then studied 12 hours later. Representative scatter plots depicting the proportion of live CD45$^+$ BAL cells that were CD11b$^+$Ly6G$^+$. **(B)** Quantification of BAL neutrophils, absolute count. **(C)** KC in cell-free BAL supernatant was measured by ELISA, concentration (pg/mL). **(D)** Quantification of lung ILC2s (live Lineage$^-$Thy1.2$^+$CD127$^+$GATA3$^+$ cells), % of lung cells. **(E)** Representative overlays of ST2 expression on lung ILC2s, % of max. **(F)** Quantification

of lung ST2^{lo}RORγt^{+} ILC2s, % of lung cells. Mean±SEM of n=5-7 **(B)**, n=6-12 **(C)**, n=6-11 **(D)**; *p<0.05, **p<0.01, ***p<0.001, #p<0.05, Two-way ANOVA with Bonferroni's multiple comparisons test (asterisk indicates air vs O_3; hashmark indicates WT vs SP-D$^{-/-}$).

Figure 7. ILC2 derived IL-17A was essential for ozone-induced neutrophilia in mice. (A-B): SP-D deficiency heightened O_3-induced IL-17A production by ILC2. **(A):** Representative scatter plots of lung IL-17A^{+} ILCs (live Lineage^{-}IL-17A^{+}CD127^{+}Thy1.2^{+} cells) that were GATA3^{+}. **(B):** Quantification of the IL-17A^{+}IL-13^{+} ILCs in the lung. % of lung cells (left panel), Lung cell count, right panel. **(C):** Quantification of lung IL-17A^{+}GATA3^{+}RORγt^{+} ILC2s, % of lung cells. **(D):** Adoptive transfer of ILC2s restored O_3-induced BAL neutrophilia: FACS sorted ILC2s from lungs of donor mice were expanded for 14 days *ex vivo* before adoptive transfer of $3x10^5$ cells into recipient Rag2/γc$^{-/-}$ mice followed by O_3 exposure. Quantification of BAL total cells and neutrophils by differential cell count of Diff-Quik stained cytospins. *p<0.05, air *vs*. O_3 with or without adoptive transfer of ILC2s; #p<0.05 Balb/c *vs.* Rag2/γc$^{-/-}$ mice exposed to O_3 (ANOVA with Tukey's post hoc test). **(E):** Correlation between % lung ILC2s and BAL neutrophils in the Rag2/γc$^{-/-}$ +O_3+ILC2 experimental group. r: Pearson's correlation coefficient. **(F):** Mice were treated with 250 µg αIgG1 or αIL-17A *i.p.* 8, 32, and 56 hours before O_3 exposure. % BAL neutrophils counted on Kwik-Diff stained cytospins from the indicated groups. Data expressed as mean±SEM of n=5-9 and are representative of at least two independent experiments. *p<0.05 (ANOVA with Tukey's post hoc test).

Figure 8. IL-17A production in lung ILC2s is driven by environmental exposures and is counteracted by SP-D. We propose that SP-D suppresses activation and

plasticity of GATA3+RORγt+ IL-13/IL-17A producing lung ILC2s, thereby protecting from eosinophilic and neutrophilic airway inflammation in COPD.

Figure E1. The distribution of pack years was similar between ILC2^{low} and ILC2^{high} COPD patients. The number of pack years the healthy, ILC2^{low} and ILC2^{high} COPD subjects smoked is depicted.

Figure E2. Mouse lung ILC2 sort purity. Representative scatter plots of pre- and post-sort ILC2s. Lung ILC2s were gated as live CD45^{+}Lineage^{-}Thy1.2^{+}CD25^{+}ST2^{+} cells.

Table 1. Characteristics of Healthy and COPD ILC2^{Low} and COPD ILC2^{High} Subjects			
Clinical Data	Healthy Subjects (n=12)	COPD ILC2^{Low} Subjects (n=7)	COPD ILC2^{High} Subjects (n=8)
Age, years	40 ± 3	70 ± 6	66 ± 3
Female sex, n (%)	6 (50)	1 (17)	5 (56)
Body mass index, kg/m^2	23 ± 2	30 ± 4	28 ± 3
Smoking history, number of pack years	0	51 ± 22	62 ± 8
SpO_2, %	100 ± 0.4	97 ± 0.9	96 ± 0.7
Modified Medical Research Council (mMRC) Scale	0.2 ± 0.2	2.0 ± 0.6	2.0 ± 0.3
COPD Assessment Test (CAT)	4.5 ± 2	17.2 ± 4	20 ± 3
6-minute walk test, meters covered	620 ± 45	396 ± 56	325 ± 49
Complete Blood Counts, x10^3/µL			
Neutrophils	2.90 ± 0.30	4.97 ± 0.77	4.85 ± 0.50
Lymphocytes	1.71 ± 0.10	1.90 ± 0.32	1.59 ± 0.24
Monocytes	0.43 ± 0.03	0.62 ± 0.06	0.56 ± 0.06
Eosinophils	0.12 ± 0.02	0.20 ± 0.05	0.14 ± 0.03
Basophils	0.04 ± 0.01	0.05 ± 0.02	0.06 ± 0.02

Table 1. Characteristics of healthy subjects and patients with ILC2^{low} and ILC2^{high} COPD sputum. Clinical data and complete blood counts (cells x10^3/µL) of n=12 healthy subjects and COPD patients with ILC2^{low} (n=7) and ILC2^{high} (n=8; defined as more than 1427 ILC2/mL) sputum. Data are presented as mean ± SEM.

Table 2. Regression models for clinical characteristics in COPD			
Outcome variable	Predictor variable	Unadjusted model	Adjusted (age) model
FEV_1, % predicted	Sputum ILC2s	-21.7 (7.02, -3.09) p=0.0053	-17.4 (6.51, -2.67) p=0.014
FVC, % predicted	Sputum ILC2s	-10.7 (5.92, -1.81) p=0.083	-8.63 (6.03, -1.43) p=0.17
CAT score	Sputum ILC2s	7.09 (2.82, 2.52) p=0.019	5.63 (2.72, 2.07) p=0.051
Sputum neutrophils	Sputum ILC2s	1.37 (0.38, 3.61) p=0.0015	1.25 (0.39, 3.21) p=0.0042
Sputum eosinophils	Sputum ILC2s	10.46 (3.62, 2.88) p=0.0086	8.45 (3.46, 2.44) p=0.023

Table 2. Regression models for clinical characteristics in COPD. FEV_1, (% predicted), FVC (% predicted), and CAT score were analyzed by linear regression. Sputum neutrophils and eosinophils were analyzed by logistic regression. Data are presented as a β coefficient or odds ratio, with 95% confidence interval and p value.

Figure 1.

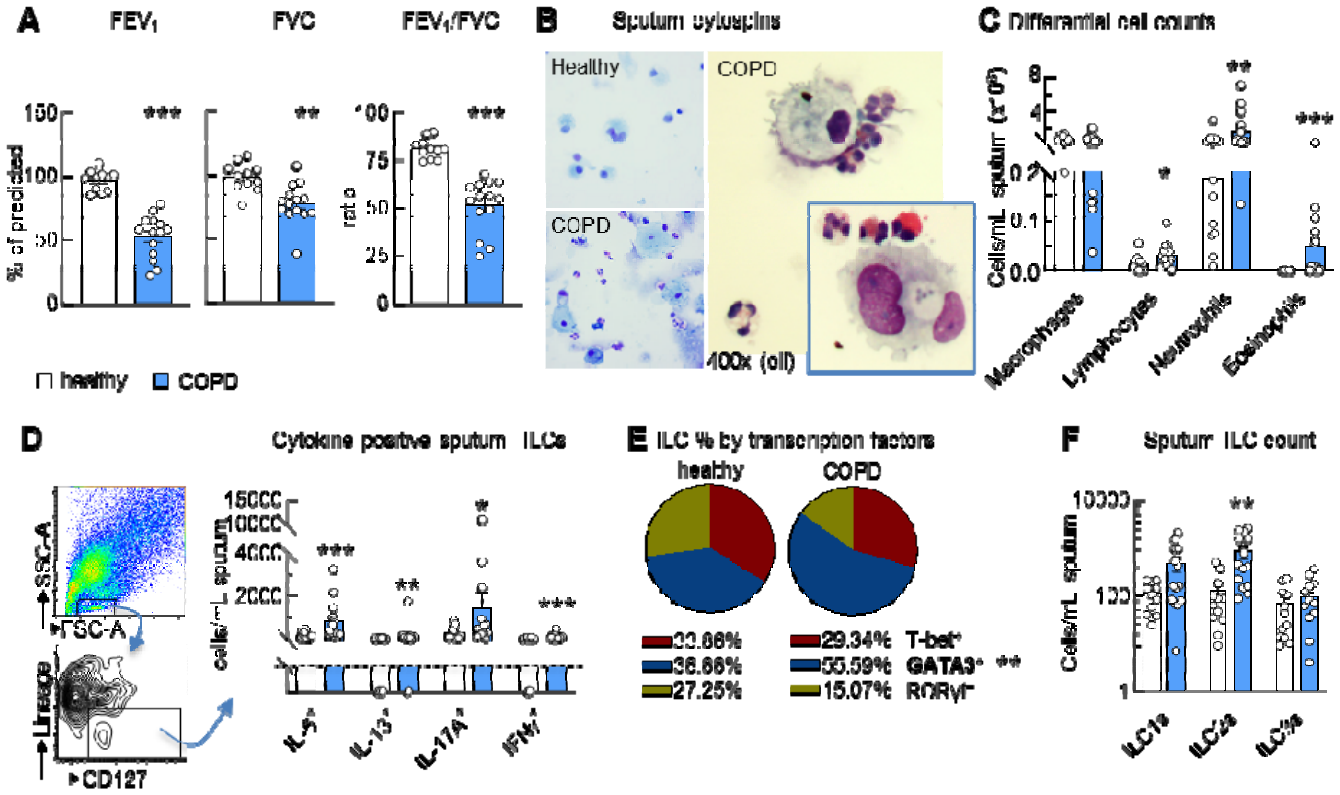
A
FEV1
FVC
FEV1/FVC
% of predicted
ratio
healthy
COPD
B
Sputum cytospins
Healthy
COPD
COPD
400x (oil)
C
Differential cell counts
Cells/mL sputum
Macrophages
Lymphocytes
Neutrophils
Eosinophils
D
Cytokine positive sputum ILCs
SSC-A
FSC-A
Lineage
CD127
cells/mL sputum
IL-5+
IL-13+
IL-17A+
IFNγ+
E
ILC % by transcription factors
healthy
COPD
29.34% T-bet+
55.59% GATA3+
15.07% RORγt+
F
Sputum ILC count
Cells/mL sputum
ILC1s
ILC2s
ILC3s

Figure 2.

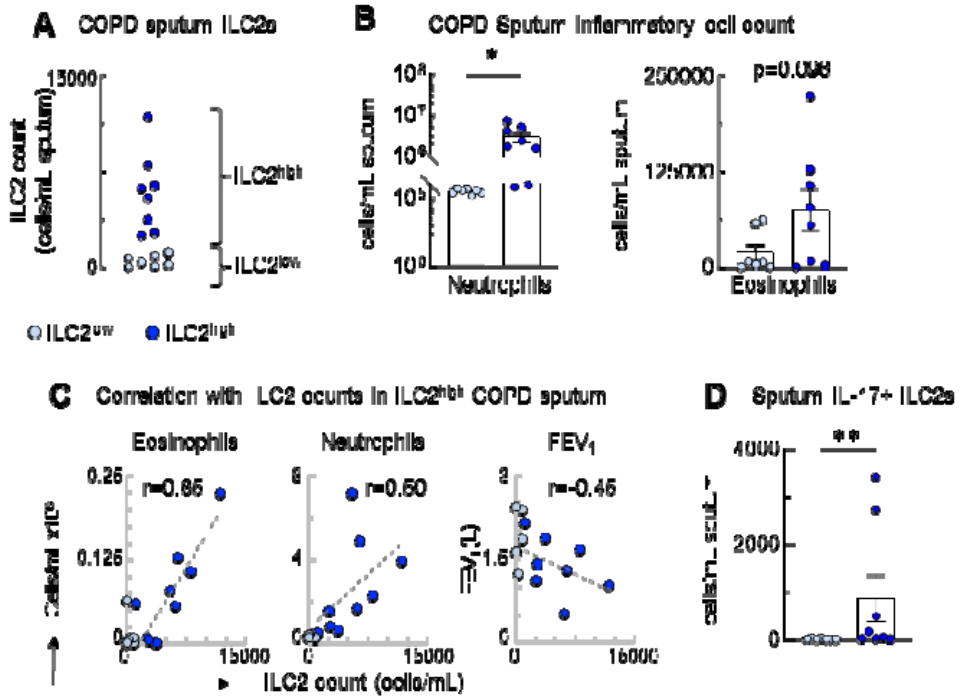
A COPD sputum ILC2s
ILC2 count (cells/mL sputum)
15000
0
ILC2high
ILC2low
ILC2low
ILC2high
B COPD Sputum Inflammatory cell count
*
Neutrophils
250000
125000
0
Eosinophils
C Correlation with ILC2 counts in ILC2high COPD sputum
Eosinophils
r=0.85
0.25
0.125
Neutrophils
r=0.50
FEV1
r=-0.45
ILC2 count (cells/mL)
D Sputum IL-17+ ILC2s
**
4000
2000
0

Figure 3.

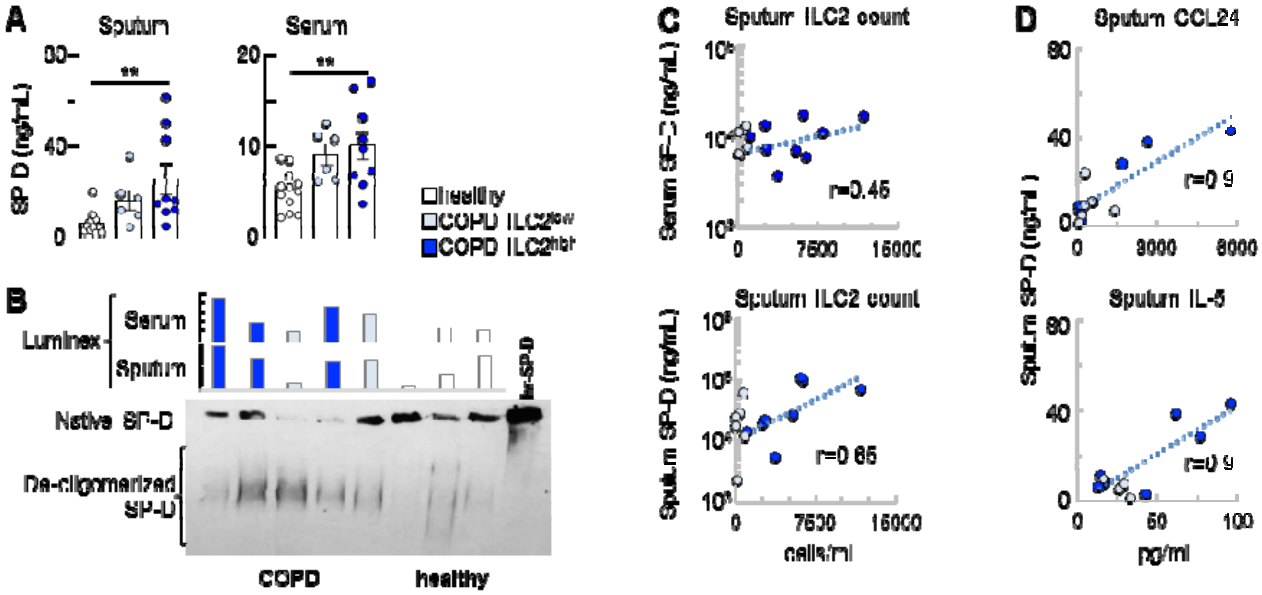
A
Sputum
Serum
SP-D (ng/mL)
**
**
healthy
COPD ILC2low
COPD ILC2high
B
Luminex
Serum
Sputum
Native SP-D
De-oligomerized SP-D
COPD
healthy
C
Sputum ILC2 count
Serum SP-D (ng/mL)
r=0.45
Sputum ILC2 count
Sputum SP-D (ng/mL)
r=0.65
cells/ml
D
Sputum CCL24
Sputum SP-D (ng/ml)
Sputum IL-5
pg/ml

Figure 4.

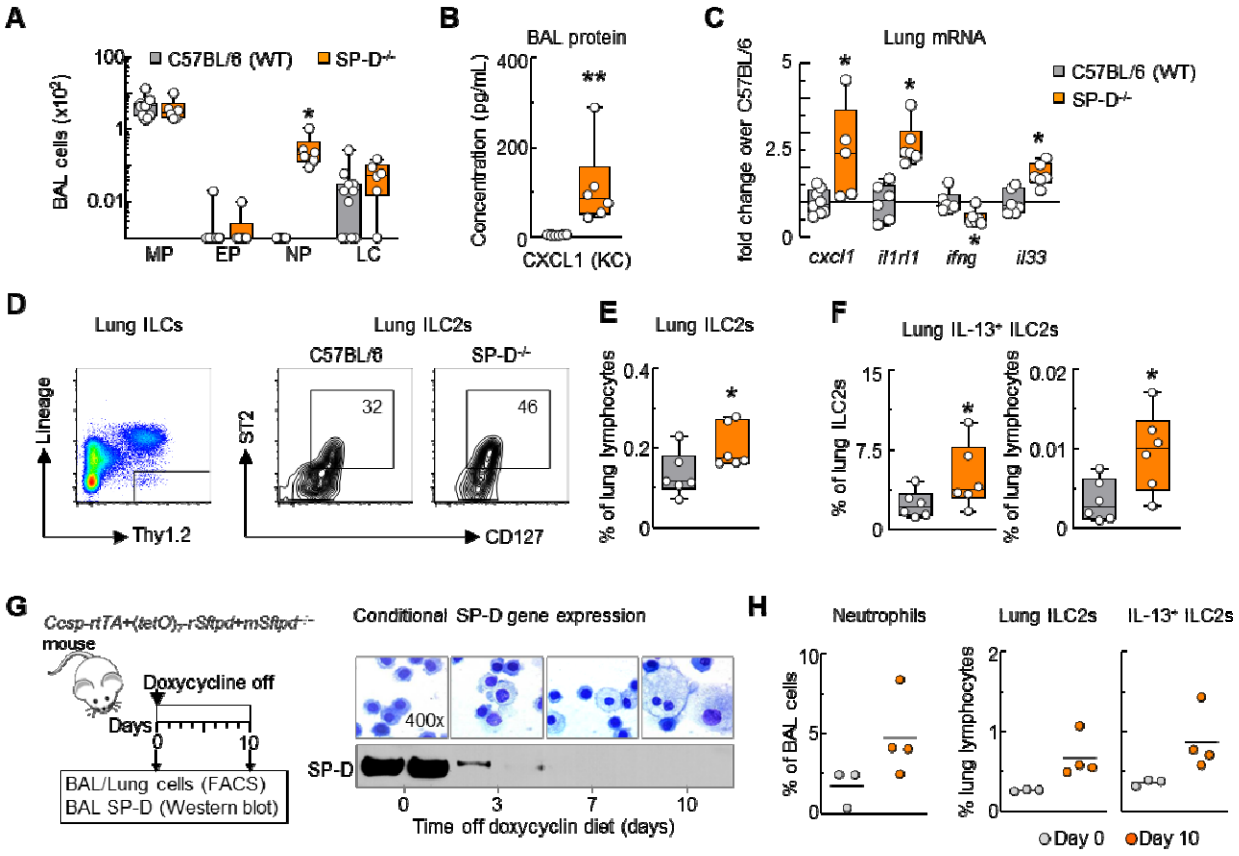
A
C57BL/6 (WT)
SP-D-/-
BAL cells (x10^3)
100
1
0.01
MP
EP
NP
LC
B
BAL protein
Concentration (pg/mL)
400
200
0
CXCL1 (KC)
C
Lung mRNA
fold change over C57BL/6
5
2.5
0
cxcl1
il1rl1
ifng
il33
D
Lung ILCs
Lung ILC2s
C57BL/6
SP-D-/-
Lineage
Thy1.2
ST2
CD127
32
46
E
Lung ILC2s
% of lung lymphocytes
0.4
0.2
0
F
Lung IL-13+ ILC2s
% of lung ILC2s
15
7.5
0
% of lung lymphocytes
0.02
0.01
0
G
Ccsp-rtTA+(tetO)7-rSftpd+mSftpd-/-
mouse
Doxycycline off
Days
0
10
BAL/Lung cells (FACS)
BAL SP-D (Western blot)
Conditional SP-D gene expression
400x
SP-D
0
3
7
10
Time off doxycyclin diet (days)
H
Neutrophils
Lung ILC2s
IL-13+ ILC2s
% of BAL cells
10
5
0
% lung lymphocytes
2
1
0
Day 0
Day 10

Figure 5.

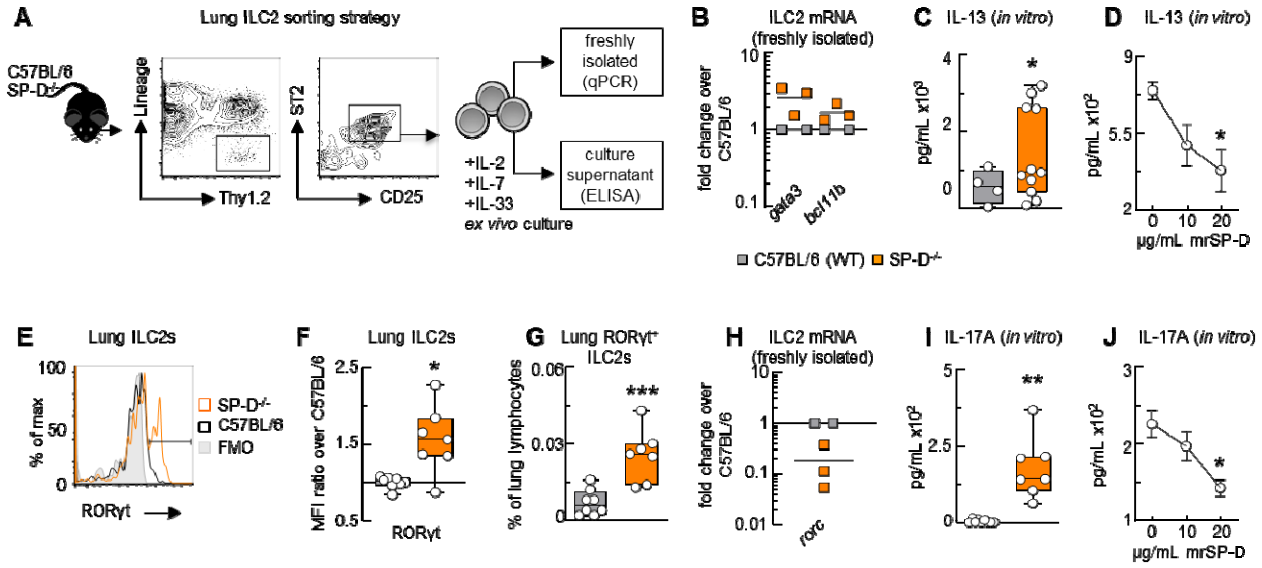
A
Lung ILC2 sorting strategy
C57BL/6
SP-D-/-
Lineage
Thy1.2
ST2
CD25
freshly isolated (qPCR)
culture supernatant (ELISA)
+IL-2
+IL-7
+IL-33
ex vivo culture
B
ILC2 mRNA (freshly isolated)
fold change over C57BL/6
gata3
bcl11b
C
IL-13 (in vitro)
pg/mL x10³
D
IL-13 (in vitro)
pg/mL x10²
µg/mL mrSP-D
C57BL/6 (WT)
SP-D-/-
E
Lung ILC2s
% of max
SP-D-/-
C57BL/6
FMO
RORγt
F
Lung ILC2s
MFI ratio over C57BL/6
RORγt
G
Lung RORγt+ ILC2s
% of lung lymphocytes
H
ILC2 mRNA (freshly isolated)
fold change over C57BL/6
rorc
I
IL-17A (in vitro)
pg/mL x10²
J
IL-17A (in vitro)
pg/mL x10²
µg/mL mrSP-D

Figure 6.

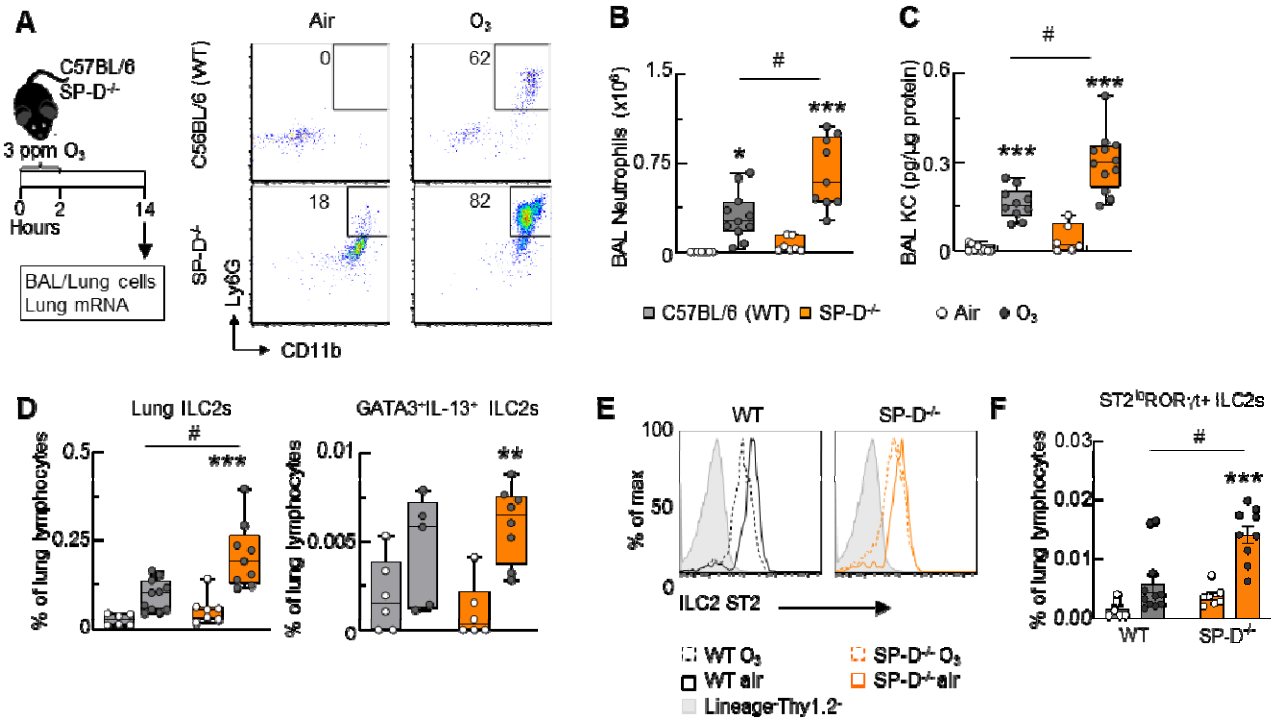
A
C57BL/6
SP-D-/-
3 ppm O3
0 2 14
Hours
BAL/Lung cells
Lung mRNA
Air
O3
C56BL/6 (WT)
SP-D-/-
0
62
18
82
Ly6G
CD11b
B
BAL Neutrophils (x10^6)
1.5
0.75
0
#
*
***
C
BAL KC (pg/µg protein)
0.6
0.3
0
#
***
***
C57BL/6 (WT)
SP-D-/-
Air
O3
D
Lung ILC2s
GATA3+IL-13+ ILC2s
% of lung lymphocytes
0.5
0.25
0
#
***
0.01
0.005
0
**
E
WT
SP-D-/-
% of max
100
50
0
ILC2 ST2
WT O3
WT air
Lineage-Thy1.2-
SP-D-/- O3
SP-D-/- air
F
ST2bRORγt+ ILC2s
% of lung lymphocytes
0.03
0.02
0.01
0.00
#
***
WT
SP-D-/-

Figure 7.

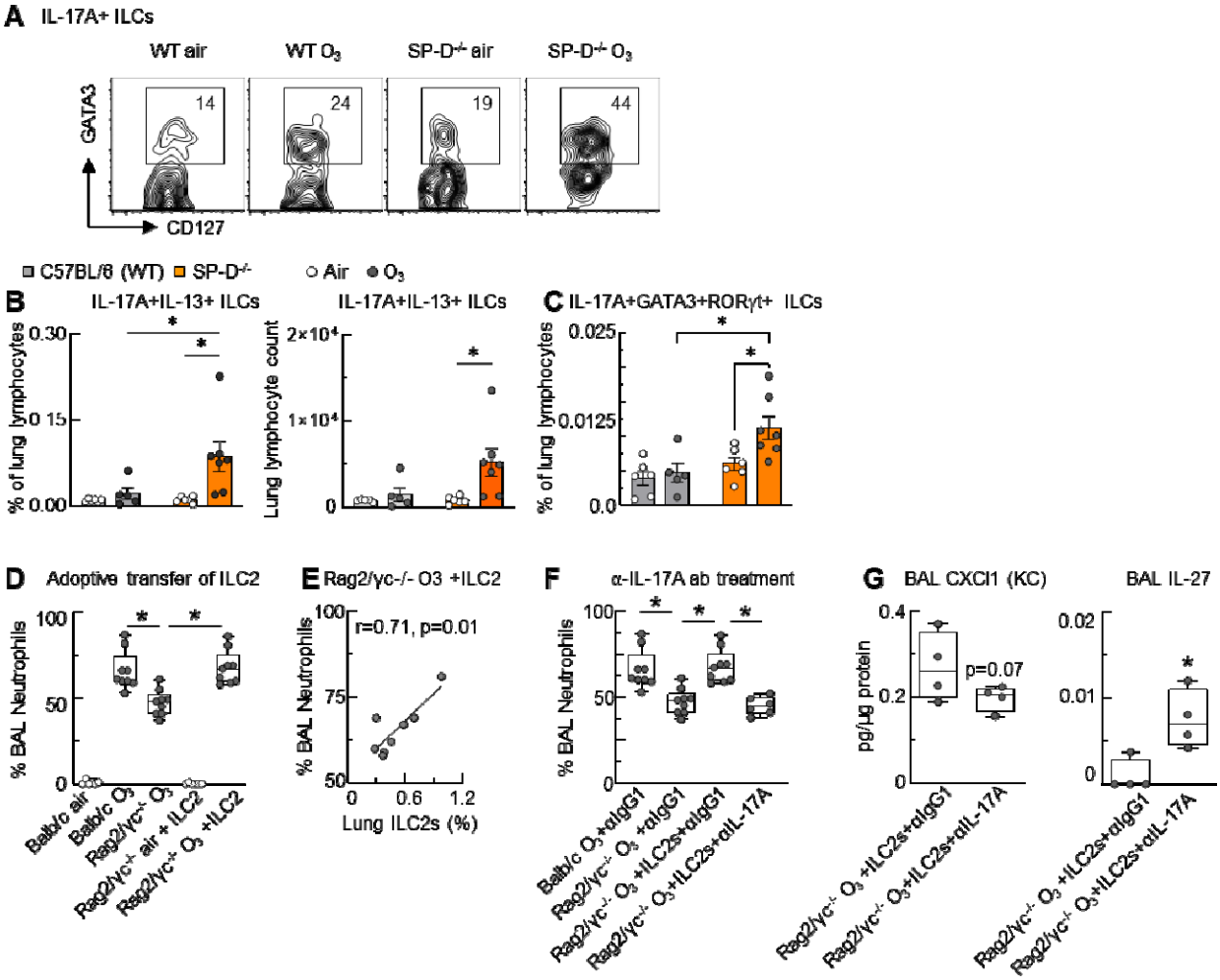
A IL-17A+ ILCs
WT air
WT O3
SP-D-/- air
SP-D-/- O3
GATA3
CD127
14
24
19
44
C57BL/6 (WT)
SP-D-/-
Air
O3
B IL-17A+IL-13+ ILCs
% of lung lymphocytes
IL-17A+IL-13+ ILCs
Lung lymphocyte count
C IL-17A+GATA3+RORγt+ ILCs
% of lung lymphocytes
D Adoptive transfer of ILC2
% BAL Neutrophils
Balb/c air
Balb/c O3
Rag2/γc-/- O3
Rag2/γc-/- air + ILC2
Rag2/γc-/- O3 +ILC2
E Rag2/γc-/- O3 +ILC2
r=0.71, p=0.01
% BAL Neutrophils
Lung ILC2s (%)
F α-IL-17A ab treatment
% BAL Neutrophils
Balb/c O3+aIgG1
Rag2/γc-/- O3 +aIgG1
Rag2/γc-/- O3 +ILC2s+aIgG1
Rag2/γc-/- O3+ILC2s+aIL-17A
G BAL CXCl1 (KC)
pg/μg protein
p=0.07
Rag2/γc-/- O3 +ILC2s+aIgG1
Rag2/γc-/- O3+ILC2s+aIL-17A
BAL IL-27
Rag2/γc-/- O3 +ILC2s+aIgG1
Rag2/γc-/- O3+ILC2s+aIL-17A
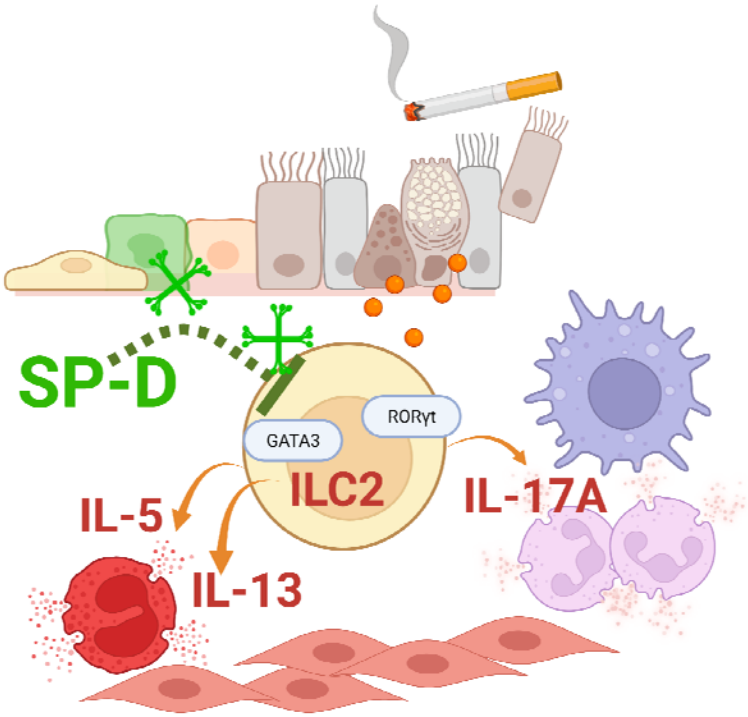
Figure 8.